Adhesion Properties of Free-Standing Hydrophobin Bilayers Supporting Information

Hendrik Hähl,*,† Jose Nabor Vargas,† Michael Jung,† Alessandra Griffo,‡ Päivi Laaksonen,‡ Michael Lienemann,¶ Karin Jacobs,† Ralf Seemann,† and Jean-Baptiste Fleury*,†

†*Department of Experimental Physics, Saarland University, D-66123, Saarbrücken, Germany*

‡*Department of Bioproducts and Biosystems BIO², Aalto University, P.O. Box 16100, 00076 Aalto, Finland*

¶*VTT Technical Research Centre of Finland Ltd., Tietotie 2, 02150 Espoo, Finland*

E-mail: h.haehl@physik.uni-saarland.de; jean-baptiste.fleury@physik.uni-saarland.de

Supplementary experimental data

In tables S1 and S2, contact angle data from measurements in the microfluidic channels are given. From these data, the bilayer tension and the bilayer adhesion energies presented in Figures 4, 5, and S1 were calculated using Eq. (1) und (2), respectively.

Figure S1 displays the tension values for bilayers from the different HFBI mutants (a) as well as from hydrophilic core bilayers from HFBI with buffer solution with increased salt concentration (b). These values correspond to the adhesion energies shown in Figure 5 in the main text.

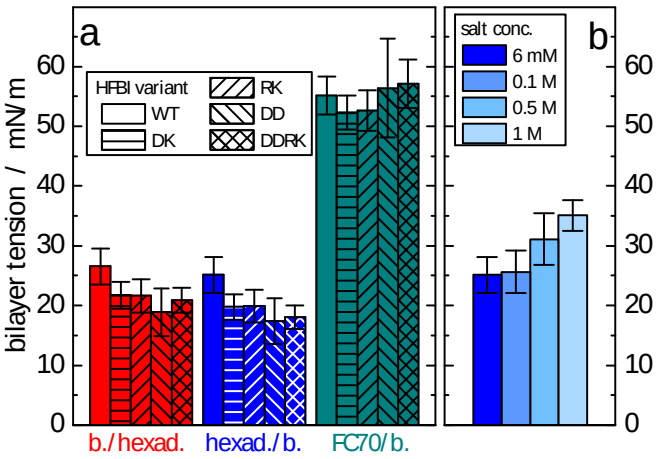

Figure S1: Bilayer tension values Γ: a) Bilayers of HFBI mutants at the interfaces buffer/hexadecane (h'phobic core, red bars), hexadecane/buffer (h'philic core, blue bars), and FC70/buffer (h'philic core, green bars). b) Hydrophilic core HFBI bilayers at the $C_{16}H_{34}$/buffer interface with varied salt concentration in the buffer phase. As described in the main text, the differences between different mutants or different salt concentrations are explained by the variation in the respective interfacial tension γ (see Tables 1 and 2 in the main text).

Calculation of the van der Waals interaction energy

To approximately derive the magnitude of the van der Waals (vdW) interaction between two protein layers, strategies for applying Lifshitz' continuum theory were used that are nicely compiled and described by Parsegian[1]. First, all media in the system were regarded as purely dielectric. Moreover, since all distances between the interacting interfaces in our system

Table S1: Experimental values for HFBI and HFBII from bilayer contact angle measurements for different phase combinations. The ionic strength of the buffer was 6 mM.

phases (finger/flow)	bilayer core	bilayer angle 2θ					
		HFBI	HFBII	HFBI-DK	HFBI-RK	HFBI-DD	HFBI-DDRK
air/buffer	hydrophilic	$41° \pm 5°$	$36° \pm 6°$	−−	−−	−−	−−
hexadecane/buffer	hydrophilic	$50° \pm 3°$	$60° \pm 4°$	$60° \pm 3°$	$58° \pm 3°$	$59° \pm 4°$	$70° \pm 4°$
FC70/buffer	hydrophilic	$36° \pm 3°$	$45° \pm 4°$	$42° \pm 3°$	$40° \pm 4°$	$40° \pm 4°$	$46° \pm 3°$
buffer/air	hydrophobic	$32° \pm 2°$	$43° \pm 2°$	−−	−−	−−	−−
buffer/hexadecane	hydrophobic	$33° \pm 2°$	$35° \pm 4°$	$37° \pm 3°$	$37° \pm 2°$	$38° \pm 4°$	$37° \pm 3°$
buffer/FC70	hydrophobic	$23° \pm 2°$	$26° \pm 5°$	−−	−−	−−	−−

Table S2: Experimental values for HFBI from bilayer contact angle measurements in a hexadecane/buffer system for different ionic strengths of the buffer (see also fig. 5 in the main text.

ionic strength I / mM	bilayer angle 2θ
100	$51° \pm 3°$
500	$54° \pm 2°$
1000	$60° \pm 2°$

are below 10 nm, retardation due to finite velocity of light was neglected. Finally, the thickness of the protein films (ca. 3 nm) is much larger than the distance l between the two films (shortly before or in "contact", i.e. well below 1 nm). Therefore the contribution of the interfaces between protein and outer solution to the overall vdW interaction is small and can be estimated to be less than 15 % at $l = 1$ nm and already less than 3 % at $l = 0.3$ nm. Consequently, the system was simplified as two half spaces of protein (index 1 and 2) interacting across a medium m, which can be air, oil, or water. Then, the free energy of interaction ΔG_{vdW} as a function of l can be written in the Hamaker form as

$$\Delta G_{\mathrm{vdW}}(l) = -\frac{k_{\mathrm{B}}T}{8\pi l^2} A_{1\mathrm{m}2} \,, \tag{1}$$

where k_{B} is the Boltzmann constant and T the absolute temperature. The Hamaker coefficient for the interaction between the two interfaces $\mathsf{1m}$ and $\mathsf{m2}$ is thereby given as

$$A_{1\mathrm{m}2} = {\sum_{n=0}^{\infty}}' \sum_{q=1}^{\infty} \frac{(\Delta_{1\mathrm{m}}\Delta_{2\mathrm{m}})^q}{q^3} \tag{2}$$

$$\text{with} \qquad \Delta_{ij} = \frac{\varepsilon_i(\mathrm{i}\xi_n) - \varepsilon_j(\mathrm{i}\xi_n)}{\varepsilon_i(\mathrm{i}\xi_n) + \varepsilon_j(\mathrm{i}\xi_n)} \tag{3}$$

evaluated at the Matsubara frequencies $\xi_n = n\, 2\pi k_{\mathrm{B}}T/\hbar$. The prime in the first summation in eq. (2) indicates that the first term is to be multiplied by 1/2. In the case of water as medium (m → w), a screening of this zero-frequency term due to ions in the solution has to be inserted so that the Hamaker coefficient becomes

$$A_{1\mathrm{w}2} = \frac{1}{2}\sum_{q=1}^{\infty} \frac{(\Delta_{1\mathrm{w}}\Delta_{\mathrm{w}2})^q}{q^3}\left(1 + \frac{2l}{\lambda_{\mathrm{D}}}\right)\mathrm{e}^{-2l/\lambda_{\mathrm{D}}} + \sum_{n=1}^{\infty}\sum_{q=1}^{\infty} \frac{(\Delta_{1\mathrm{w}}\Delta_{\mathrm{w}2})^q}{q^3} \,, \tag{4}$$

where λ_{D} is the Debye screening length.

The dielectric functions $\varepsilon(\mathrm{i}\xi)$ were approximated with the damped oscillator form

$$\varepsilon(\mathrm{i}\xi) = 1 + \sum_j \frac{d_j}{1 + \xi\tau_j} + \frac{f_j}{\omega_j^2 + g_j\xi + \xi^2} \,, \tag{5}$$

where the coefficients derived from spectral data where taken from Parsegian's book [1] in the case of water and oil (for which the values for tetradecane were used). Since not enough spectral data for HFBI exist, coefficients for the protein bovine serum albumin (BSA) taken from Roth et al. [2] were used. Also the protein ori-

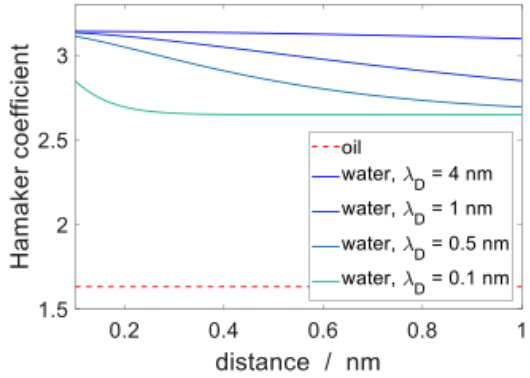

Figure S2: Hamaker coefficient as function of the distance of the two interfaces as calculated from eq. (4) for oil and from eq. (6) for the buffer solutions.

entation is neglected. Since the protein always orients such that the less polarizable groups are exposed to the less polarizable medium and vice versa, this simplification might lead to a slight overestimation of the interaction strength.

In our numerical calculation, the sums were evaluated until $q = 5$ and $n = 1000$ (as recommended by Parsegian[1]). Tests with higher numbers for q and n were also performed but no significant changes were observed. The calculated Hamaker coefficient for the interaction across oil (eq. 4) is a constant value of 1.63. For the interaction across the electrolyte solution, values between 2.67 and 3.14 were computed (see Fig. S2).

The calculated potentials are shown in fig.5 of the main text. For small distances, the free energy approaches values that compare well with the measured adhesion energy of the protein bilayers. Also a smaller interaction for oil as medium than for water as medium is found. Higher ionic strength, however, does not influence the vdW interaction across water significantly at the probed distances. In sum, the qualitative behavior resembles the one found in the experiments.

For a more quantitative description, however, the whole interaction potential, i. e. electrostatic, steric, and possibly solvation and hydration forces, has to be considered. Only then, a contact point can be defined and from that the adhesion energy can be extracted. Still, this would be a continuum description and as such suffering from its limitations when describing the contact of two layers consisting of macromolecules.

Discussion of the pendant drop and contact angle measurements with respect to the elasticity of the interface

As could be shown by several authors, fully formed interfacial protein films from class II hydrophobins as HFBI and HFBII exhibit a dilatational and shear elasticity[3456]. This elasticity leads to effects like buckling in Langmuir trough measurements[4] or elongated droplets and wrinkling at the droplet neck in pendant drop measurements[789]. The elasticity makes the measurement of the surface energy complicated since in such systems, the surface stress is composed of the (thermodynamical) isotropic interfacial tension and additional mechanical contributions[1011]. As a result, the Laplace model for the droplet shape analysis is not applicable anymore, which is also indicated by a large fit error[59].

In our measurements, we tried to avoid the solidification of the interface and the concomitant problems concerning the interfacial tension. In the pendant droplet measurements, this was done by a slight increase in the droplet volume. This also mimics the situation in the microfluidic channels where the fingers also increase in volume (and hence also the surface area increases) before they are contacted. With the described procedure, we did not record an increase in the fit error and did not record deformations in the microfluidic channels which would result from an elastic behavior. The obtained values for the interfacial tension have to be seen, however, as an upper approximation of the surface energy of the interface. Therefore additional experiments as the one described below were performed in order to validate at least the order of magnitude of the obtained adhesion energies.

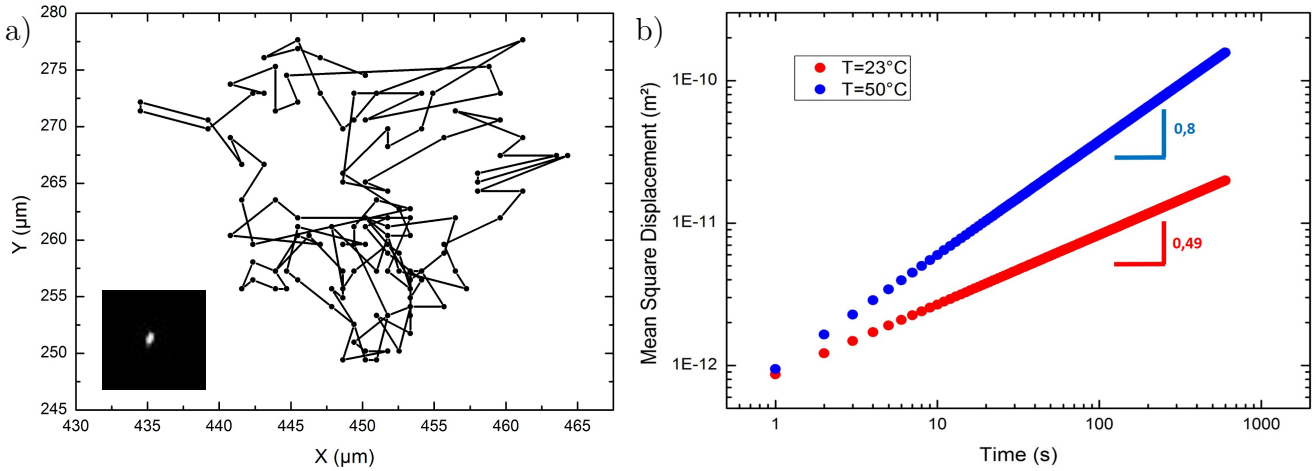

Figure S3: a) Trajectory from the motion of an oil droplet covered with fluorescent protein (HFBI-GFP) and observed with an epifluorescent microscope. In insert, a picture of the corresponding oil droplet (in bright). b) Mean square displacement of HFBI-WT covered and stabilized oil droplets on the protein covered bottom of the PDMS chip. The slope of the curves indicates a subdiffusive behaviour of the oil droplets. This behaviour is less pronounced for an elevated temperature of about 50 °C.

Consequence of the weak protein-protein interaction on the mobility of small droplets

Since the adhesion energy between the bilayer sheets is only in the range of k_BT, thermal fluctuations should have an influence. To be able to observe this influence, another set of experiments has been performed. In a PDMS chip prefilled with FC70, a large droplet of buffered solution with a HFBI-WT concentration of 5 µM was introduced into a reservoir (for a description of the whole microfluidic chip's shape, see Hein et al.[12]) filling it nearly completely and leave to rest. After 15–20 minutes, the oil between channel walls and the droplet's interface is drained off and the adsorption of the hydrophobins to the PDMS fixes the droplet to the wall of the chip. Moreover, during that time, small FC70 droplets with diameters in the range from 1–5 µm appear inside the large droplet due to spontaneous emulsification. Since FC70 is about two times denser than water, these small oil droplets sink to the bottom of the large droplet, where they perform a diffusive 2D motion.

To confirm that the small oil droplets are covered by hydrophobins and to accurately track the diffusive motion traces, an additional experiment with fluorescent hydrophobins, i.e. a HFBI fusion protein with an attached GFP (green fluorescent protein) domain (GFP-HFBI)[13], was performed. With these proteins in the buffer, the small oil droplets as well as the interface of the large buffer droplet showed a strong fluorescence signal in epifluorescence microscopy under laser excitation ($\lambda = 473$ nm). The trajectory of such a droplet is presented in figure S3 a). Since the presence of the GFP domain, however, certainly influences the interaction between the proteins, the wild type form of HFBI was used in the experiments described in the following. Even without the fluorescence, it is possible to record the trajectory of individual droplets.

Since the small oil droplets are protein covered and sink to the bottom of the large droplet, they will form a local bilayer with the protein coating of the large buffer droplet. As the adhesion energy of the bilayers is rather weak (in the range of k_BT), the droplets are not immobilized but rather hinder the two-dimensional Brownian motion. Interestingly, the recorded Brownian motion analysis at room temperature shows for the small droplets' mean square displacement at the large droplet's bottom a clear subdiffusive behavior with $\langle \Delta X^2 \rangle \propto t^\alpha$, where $\alpha \approx 0.5$ (see figure S3). This subdif-

fuse behavior may be attributed to the adhesive interaction energy between the HBFI monolayer at the large buffer droplet's interface and the HBFI monolayer at the oil droplet's surface. Here, the hydrophilic parts of the HFBI molecules interact, similar to the situation in the hydrophilic core bilayer. If we consider the protein pair interaction energy for this situation, which is $2.6(8)\,k_{\mathrm{B}}T$, this energy should be enough to temporally trap the droplets in contact with a protein monolayer. It is, however, not enough to allow a permanent trapping of the droplets. To test this hypothesis, the Brownian motion of the droplets was recorded with an increased sample temperature of 50 °C. If the motion was only due to a diffusive process, its mean square displacement should should not change its power law behavior with temperature. Instead, the droplet motion seems to recover a normal diffusion ($\alpha \approx 0.8$). From this simple test, it can be concluded that the pair interaction energy between HBFI molecules is in fact of the order of few $k_{\mathrm{B}}T$, which corroborates the results from the contact angle measurements.

References

(1) Parsegian, V. A. *Van der Waals forces*; Cambridge: New York, 2006.

(2) Roth, C. M.; Neal, B.; Lenhoff, A. M. Van der Waals interactions involving proteins. *Biophysical Journal* **1996**, *70*, 977–987.

(3) Cox, A. R.; Cagnol, F.; Russell, A. B.; Izzard, M. J. Surface properties of class II hydrophobins from Trichoderma reesei and influence on bubble stability. *Langmuir* **2007**, *23*, 7995–8002.

(4) Aumaitre, E.; Vella, D.; Cicuta, P. On the measurement of the surface pressure in Langmuir films with finite shear elasticity. *Soft Matter* **2011**, *7*, 2530–2537.

(5) Alexandrov, N. A.; Marinova, K. G.; Gurkov, T. D.; Danov, K. D.; Kralchevsky, P. A.; Stoyanov, S. D.; Blijdenstein, T. B. J.; Arnaudov, L. N.; Pelan, E. G.; Lips, A. Interfacial layers from the protein HFBII hydrophobin: dynamic surface tension, dilatational elasticity and relaxation times. *Journal Of Colloid And Interface Science* **2012**, *376*, 296–306.

(6) Lienemann, M.; Gruner, M. S.; Paananen, A.; Siika-Aho, M.; Linder, M. B. Charge-based engineering of hydrophobin HFBI: effect on interfacial assembly and interactions. *Biomacromolecules* **2015**, *16*, 1283–1292.

(7) Szilvay, G. R.; Paananen, A.; Laurikainen, K.; Vuorimaa, E.; Lemmetyinen, H.; Peltonen, J.; Linder, M. B. Self-assembled hydrophobin protein films at the air-water interface: Structural analysis and molecular engineering. *Biochemistry* **2007**, *46*, 2345–2354.

(8) Knoche, S.; Vella, D.; Aumaitre, E.; Degen, P.; Rehage, H.; Cicuta, P.; Kierfeld, J. Elastometry of deflated capsules: elastic moduli from shape and wrinkle analysis. *Langmuir* **2013**, *29*, 12463–12471.

(9) Danov, K. D.; Stanimirova, R. D.; Kralchevsky, P. A.; Marinova, K. G.; Stoyanov, S. D.; Blijdenstein, T. B. J.; Cox, A. R.; Pelan, E. G. Adhesion of bubbles and drops to solid surfaces, and anisotropic surface tensions studied by capillary meniscus dynamometry. *Advances In Colloid And Interface Science* **2016**, *233*, 223–239.

(10) Fuller, G. G.; Vermant, J. Complex Fluid-Fluid Interfaces: Rheology and Structure. *Annual Review of Chemical and Biomolecular Engineering* **2012**, *3*, 519–543.

(11) Nagel, M.; Tervoort, T. A.; Vermant, J. From drop-shape analysis to stress-fitting elastometry. *Advances In Colloid And Interface Science* **2017**, *247*, 33–51.

(12) Hein, M.; Fleury, J.-B.; Seemann, R. Coexistence of different droplet generating instabilities: new breakup regimes of a liquid filament. *Soft Matter* **2015**, *11*, 5246–5252.

(13) Joensuu, J. J.; Conley, A. J.; Lienemann, M.; Brandle, J. E.; Linder, M. B.; Menassa, R. Hydrophobin fusions for high-level transient protein expression and purification in Nicotiana benthamiana. *Plant Physiology* **2010**, *152*, 622–633.